Geologica Acta, Vol.11, Nº 4, December 2013, 421-441
DOI: 10.1344/105.000002061
Available online at www.geologica-acta.com

geologica acta

The record of the Paleocene-Eocene thermal maximum in the Ager Basin (Central Pyrenees, Spain)

N. Minelli [1] **V. Manzi** [1,2] **M. Roveri** [1,2]

[1] **Dipartimento di Fisica e Scienze della Terra Macedonio Melloni**
Parco Area delle Scienze 157/A, 43100 Parma, Italy. Minelli E.mail: nicola.minelli@unipr.it

[2] **Alpine Laboratory of Palaeomagnetism (ALP)**
Via Madonna dei Boschi 76, 12016 Peveragno (CN), Italy

ABSTRACT

The sedimentary record straddling the Paleocene-Eocene boundary in the Ager Basin (southern Central Pyrenees) was investigated by combining facies analysis, sequence stratigraphy and stable isotope data, within an interval characterized by a great variability of depositional environments. The occurrence of the Paleocene-Eocene thermal maximum climatic anomaly is tentatively constrained by analogy with its stratigraphic range in the adjacent Tremp-Graus Basin. The main body of the carbon isotope excursion associated with this thermal maximum may be recorded by lacustrine carbonates characterized by a ~ -3‰ shift in $\delta^{13}C$ with respect to analogous deposits of Thanetian age. A similar shift is recorded between in situ and resedimented pedogenic carbonates, a feature that suggests the partial erosion of the Paleocene-Eocene boundary in the Ager Basin.

KEYWORDS | **Paleocene-Eocene thermal maximum. Southern Central Pyrenees. Isotope geochemistry.**

INTRODUCTION

The study of the Paleocene-Eocene Thermal Maximum (PETM) was extended in recent years into the southern Central Pyrenees foreland basin, where the Paleocene-Eocene boundary issue was complicated by its proximity with a continental/marine facies boundary. Schmitz and Pujalte (2003) reported that the Carbon Isotope Excursion of the Paleocene-Eocene Thermal Maximum (PETM CIE) was preserved within the continental Tremp Formation (Fm.) (*sensu* Mey *et al*., 1968) of the Tremp-Graus Basin (provinces of Lleida and Huesca, Spain), and correlated it along a continental-to-marine transect, *i.e*. from the southern Central Pyrenees domain to the deep-marine successions of the Basque-Cantabrian region. Schmitz and Pujalte (2003) and Schmitz *et al*. (2001), pointed out the regional-scale effects of the PETM, expressed by an increase in land erosion and continental runoff during the isotope excursion, driven by a stronger seasonal character of the climate.

In this paper we describe for the first time the sedimentary record of the PETM in the Ager Basin, a narrow thrust-sheet-top basin located south of the Tremp-

Graus Basin. The main aim of our work is to constrain the stratigraphic range of this thermal maximum in the Ager area and to establish a more precise correlation to the Tremp-Graus Basin. These are key elements to discuss the implications of this hyperthermal event for the regional geological evolution and for a better understanding of its impact on continental depositional systems.

The early Paleogene sedimentary successions of the Tremp-Graus and Ager basins are comparable in general litho- and physical-stratigraphic terms (Mutti *et al.*, 1988, 1994). The more or less marked differences in the distribution of sedimentary environments were mainly controlled by the local paleotopography and the overall morphostructural setting; the latter is in large part related to the early evolution of the structural high that separates them, the Montsec thrust; (Mutti *et al.*, 1985; Mutti *et al.*, 1988; Mutti *et al.*, 1994; Rosell *et al.*, 2001; López-Martínez *et al.*, 2006). For an integrated inter-basinal study, the chronostratigraphic correlation between the Tremp and Ager basins is of primary importance, given that there is no physical continuity between their respective early Paleogene successions. This is particularly important within the ~1000m-thick continental Tremp Fm. or Garumnian facies (*sensu* Rosell *et al.*, 2001, with references therein), of Maastrichtian to lower Ypresian age.

The precise location of the PETM, within the succession encompassing the interval between the late Thanetian (*sensu* Gradstein *et al.*, 2004) and the Ypresian (Paleocene-Eocene boundary interval) in the Ager Basin, represents an even more challenging issue than in the Tremp-Graus Basin, due to the greater variability of sedimentary environments and lower outcrop quality. These two conditions hamper the reconstruction of a continuous isotope record. However, the integration of facies and sequence-stratigraphic analysis with the isotope data, and the comparison with the coeval interval in the Tremp-Graus Basin, allowed an isotope characterization of some distinctive lithological units, constraining the onset of the PETM CIE to a very narrow interval.

GEOLOGICAL SETTING

The Ager Basin (Fig. 1B, C) is currently structured in an E-W trending, asymmetric syncline, the Ager Syncline (Mutti *et al.*, 1985; Mutti *et al.*, 1994), bounded by the Montsec thrust to the north and the inner anticlines of the Sierras Marginales to the south (Millà and St. Mamet anticlines). The Montsec thrust separates the Ager Basin from the Tremp-Graus Basin (Fig. 1B) and acted as a topographic high at least since the Paleocene (Mutti *et al.*, 1985; Rosell *et al.*, 2001; Muñoz, 2002). Later reactivations of this structure (Oligocene; *cf.* Muñoz, 2002, with references therein) caused overthrusting of the northern margin of the Ager Basin, so this sector is presently exposed only in a small portion. To the south, the Millà (SW) and St. Mamet (SE) anticlines outline an irregular basin margin, with a large transversal structural depression (Baronia Trough, Fig. 1C). This depression and its bounding highs were probably active since the Paleocene, as inferred from differential subsidence patterns in E-W transects (*e.g.* fig. 2 in Colombo and Cuevas, 1993; fig. 3 in Rossi, 1997b).

The most continuous outcrops are present along the northern flanks of the St. Mamet and Millà anticlines and in the Baronia Trough; they consist of rocks ranging from the Campanian to the Ypresian. During the late Paleocene the Ager Basin was filled by a succession of continental, mainly flood-plain to lacustrine deposits (Upper Tremp Fm.), interfingering with shallow-marine calcarenites, which record a number of successive transgressive events. The sea was located to the west, and flooded each time farther to the east, depicting an overall transgressive trend (Rossi, 1997a, fig. 1).

The most extensive transgressions occurred in the late Thanetian and early Ypresian (Fig. 2; Ferrer *et al.*, 1973; Rossi, 1997b). These two events flooded the entire basin, and the younger one caused the establishment of marine conditions up to the middle-late Ypresian. The older transgression (late Thanetian) was a short-lived event, ended by a relative sea-level fall marked by an exposure surface with paleokarst features (Rossi, 1997a; Rossi, 1997b) that can be easily followed throughout the southern margin of the basin. The upper Thanetian and lower Ypresian marine deposits are separated by a continental interval, which includes the Paleocene-Eocene boundary interval in the Ager Basin.

The Paleocene-Eocene thermal maximum and the Paleocene-Eocene boundary in the southern Central Pyrenees foreland basin

The PETM is a short-term episode of global warming (Kennett and Stott, 1991), driven by a massive increase of atmospheric CO_2 characterized by a very depleted $\delta^{13}C$ ratio (Carbon Isotope Excursion, CIE). The causes of this phenomenon are still uncertain, but some global and local consequences (involving environmental and biotic changes), have been outlined with clarity because of the ease of recognition of the isotope signals ($\delta^{18}O$ and $\delta^{13}C$) in sedimentary successions ranging from abyssal to continental environments (*e.g.* Kennett and Stott, 1991; Koch *et al.*, 1992).

Apart from the paleoenvironmental implications of the PETM, the isotope signal (particularly the CIE) constitutes

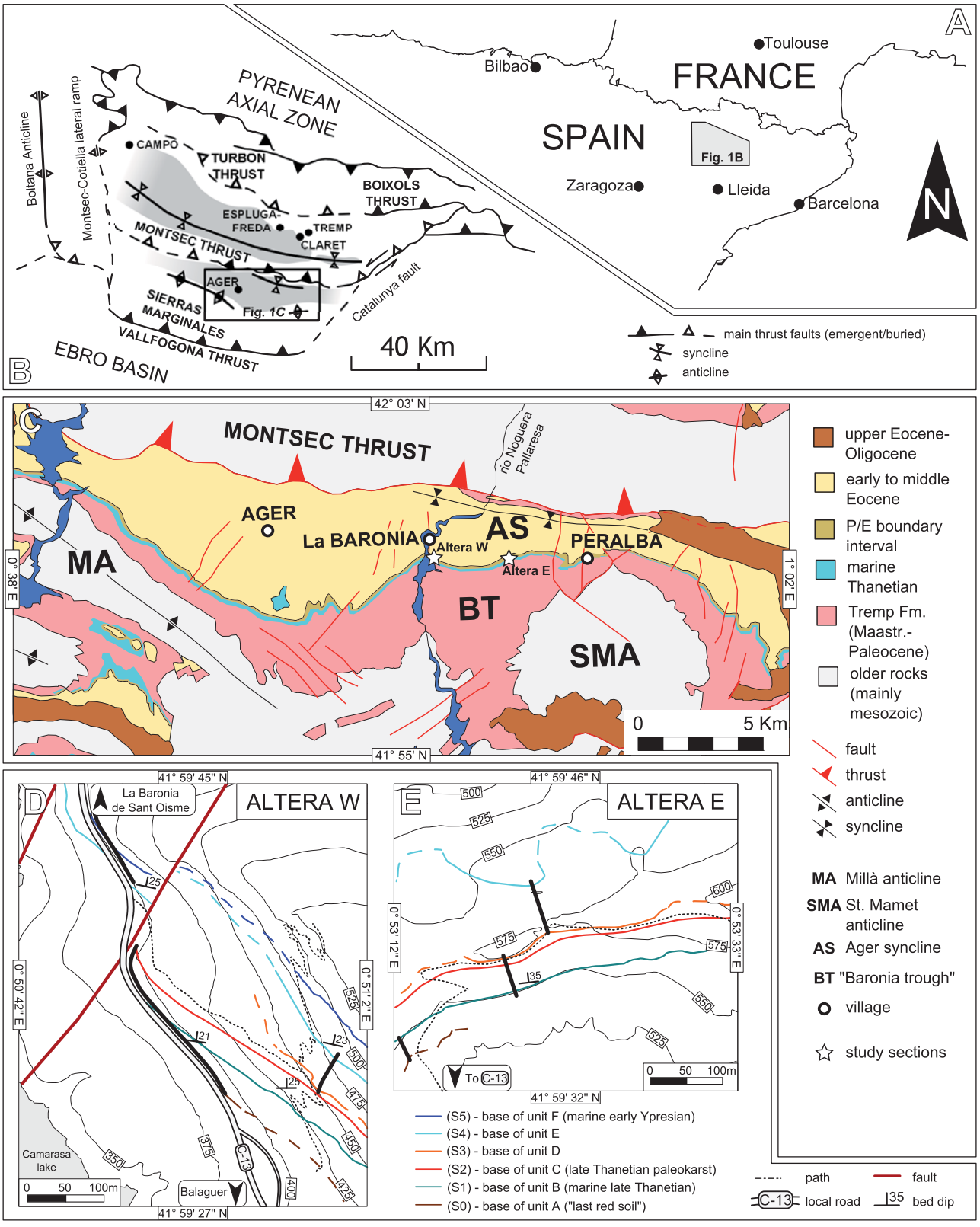

FIGURE 1 | Geological setting of this study; A) geographic location of the study area; B) Schematic geological-structural map of the southern Central Pyrenees (slightly modified after Mutti et al., 1988); the area occupied by the Ager and Tremp-Graus basins at the beginning of the Eocene are represented in grey; C) geological map of the Ager Basin, based on the Mapa Geològic de Catalunya of the Institut Geològic de Catalunya (ICG), scale 1:250,000; D, E) detailed geological maps (based on ortophotomaps, scale 1:5,000) at the study sections; topography derived from the topographic map of the Institut Cartografic de Catalunya (ICC), scale 1:5,000.

a powerful correlation tool, allowing to trace a virtually isochronous surface, and an unifying criterion for the Paleocene/Eocene boundary (Aubry *et al.*, 2007).

Tremp-Graus Basin

In the northern sector of the Tremp-Graus Basin, Schmitz and Pujalte (2003) and Schmitz and Pujalte (2007) localized the Paleocene-Eocene boundary within the upper portion of the Tremp Fm. (Claret Fm., *sensu* Pujalte and Schmitz, 2005) by recognizing the PETM isotope record in paleosol carbonate nodules in a number of sections, thus allowing to trace a continental-to-marine transect of the PETM, *i.e.* from the southern Central Pyrenees foreland basin to the basin plain deposits in the Basque-Cantabrian domain (Fig. 3). In the Esplugafreda section (*cf.* Fig. 1B) clay-mineral compositions show higher kaolinite content within the syn-PETM paleosols, suggesting an increase of land erosion during the climatic anomaly (Schmitz and Pujalte, 2003). This was explained by the occurrence of a seasonally humid climate, which contrasted with the arid conditions typically observed during the Paleocene in this region.

A striking feature related to the PETM onset is the occurrence of a distinctive tabular conglomerate unit, the Claret conglomerate at the turning point between pre- and syn-CIE $\delta^{13}C$ values (this relationship was better defined by organic matter $\delta^{13}C$ by Domingo *et al.*, 2009). Schmitz and Pujalte (2003) interpreted the Claret conglomerate as a fluvial deposit recording a major continental runoff increase (possibly enhanced by a relative sea-level fall) related to the initial PETM. Evidence for syn-PETM increased continental runoff in the Pyrenean region was also provided by Storme *et al.* (2012) in the correlative basin-plain succession of Zumaia (Basque Pyrenees). In the Tremp-Graus Basin, the PETM occurs within a small-scale depositional sequence (the Serraduy sequence of Luterbacher *et al.*, 1991; Fig. 2), which encompasses the transition from the Tremp Fm. to the overlying marine Ilerdian deposits.

In the area between the Isabena and Noguera Pallaresa valleys, the basal sequence boundary of the Serraduy sequence is represented by a discontinuous belt of channelized sandstones and conglomerates (Fig. 3), locally emphasized by a sharp change of paleosol color (from red to yellow). These deposits were interpreted as the early fill of an incised valley (*cf.* Eichenseer and Luterbacher, 1992; Baceta *et al.*, 2011). West of the Isabena river, in the area of Campo (Figs. 1B; 3), this sequence boundary is represented by a subaerial exposure surface with paleokarst features developed on upper Thanetian marine algal boundstones (*e.g.* Scheibner *et al.*, 2007; Pujalte *et al.*, 2009a). The Claret conglomerate, located a few meters

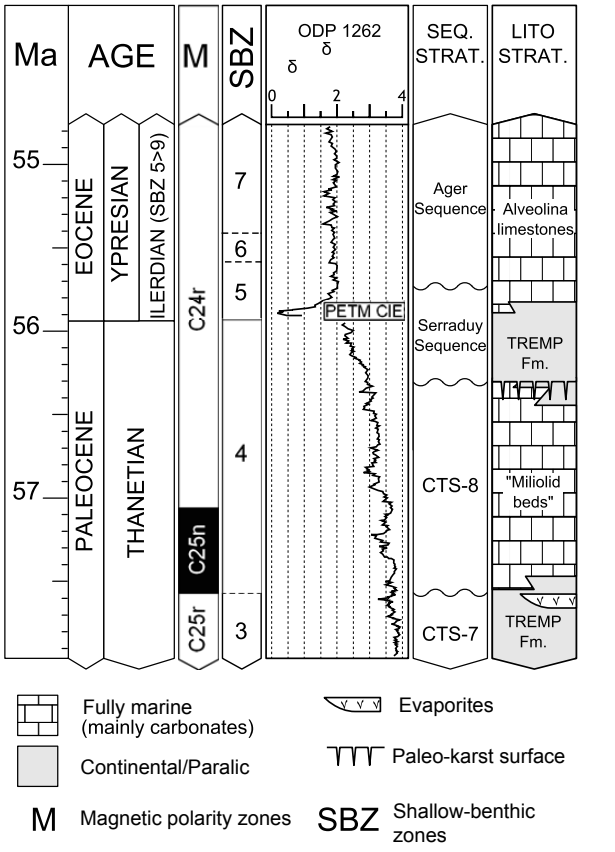

FIGURE 2 Chronostratigraphic framework of the studied interval, including the main lithostratigraphic units encountered in the Paleocene/Eocene transition in the Ager Basin. The ages of the sequence boundaries are very approximate, since they are mainly bound to benthic biozones.

above this sequence boundary, is a few-m-thick, very distinctive lithohorizon, which constitutes a basin wide keybed. To the east, the Claret conglomerate is overlain by a package of moderately pedogenized mudstones formed during the PETM (yellow paleosols of Schmitz and Pujalte, 2003), which are capped by post-PETM evaporites. Above the latter, a gradual transition from palustrine-lagoonal to fully marine deposits is observed, forming the classic lower Ypresian transgressive systems tract of the Serraduy Sequence. On the basis of Pujalte *et al.* (2009b) correlation, they concluded that the whole package of the yellow paleosols formed during a phase characterized by relative base-level rise and transgressive conditions. Despite some uncertainties in the placement of the CIE top in the Campo section and the effect of local subsidence, the continental interval between the Claret conglomerate and the marine flooding surface clearly thickens towards the east; this is consistent with a gradual eastward transgression. The upper boundary of the Serraduy sequence (not treated in this paper) coincides with a reactivation of fluvial systems, which built small deltaic complexes of lower Ypresian age (*e.g.* La Farga Fm. in Barberà *et al.*, 1997; *cf.* Eichenseer and Luterbacher, 1992).

The Serraduy sequence and its component systems tracts can be traced also in the southern margin of the Tremp-Graus Basin, including a finer-grained equivalent of the Claret conglomerate (*e.g.* Eichenseer and Luterbacher, 1992; Waehry, 1999).

Ager Basin

In the southern Ager Basin, the Paleocene-Eocene boundary interval displays some similarities with the western portion of the Tremp-Graus Basin. In particular, marine to coastal Thanetian deposits are topped in both basins by a paleokarst, suggesting the occurrence of the same sequence boundary, *i.e.* the lower boundary of the Serraduy Sequence (*e.g.* Rossi, 1997a). Also, the base of the marine Ypresian (Alveolina limestones or Cadí Fm.) roughly has the same age in both basins belonging to the Shallow-Benthic Zone 5 (SBZ 5; Serra-Kiel *et al.*, 1998), which may represent a relatively short time interval, lasting 300-400kyr. This value was obtained by Minelli (2012) by integrating the PETM record (Pujalte *et al.*, 2009b) with the available chronostratigraphic constraints of the Tremp section (Fig. 2; Pascual *et al.*, 1992; Serra-Kiel *et al.*, 1994; Serra-Kiel *et al.*, 1998; Waehry *et al.*, 1999) and with the recent early Paleogene age models (Westerhold *et al.*, 2007; Westerhold *et al.*, 2008). Since in the upper Thanetian of the Ager Basin fluvial deposits are generally poorly developed, their occurrence between the Thanetian and Ypresian marine deposits suggests a direct relationship with the period of enhanced fluvial discharge occurring during the initial PETM.

THE PALEOCENE-EOCENE BOUNDARY IN THE AGER BASIN

Study locations

We studied the interval encompassing the Paleocene-Eocene boundary in two sections located within the Baronia Trough (Fig. 1C): Altera W, located south of the village of La Baronia de Sant Oïsme (Fig. 1D), largely exposed along the C-13 roadcut; and Altera E, located along a path connecting the C-13 road with the abandoned village of Peralba, on the eastern side of the Altera hill (Fig. 1E). In the study area, beds dip roughly to the N, with an average inclination of 20°-25°, and the main stratigraphic surfaces can be reliably traced for many kilometers. The studied interval also included the upper portion of the Thanetian, in order to collect isotope data from pre-PETM strata. A description of the Paleocene-Eocene boundary interval

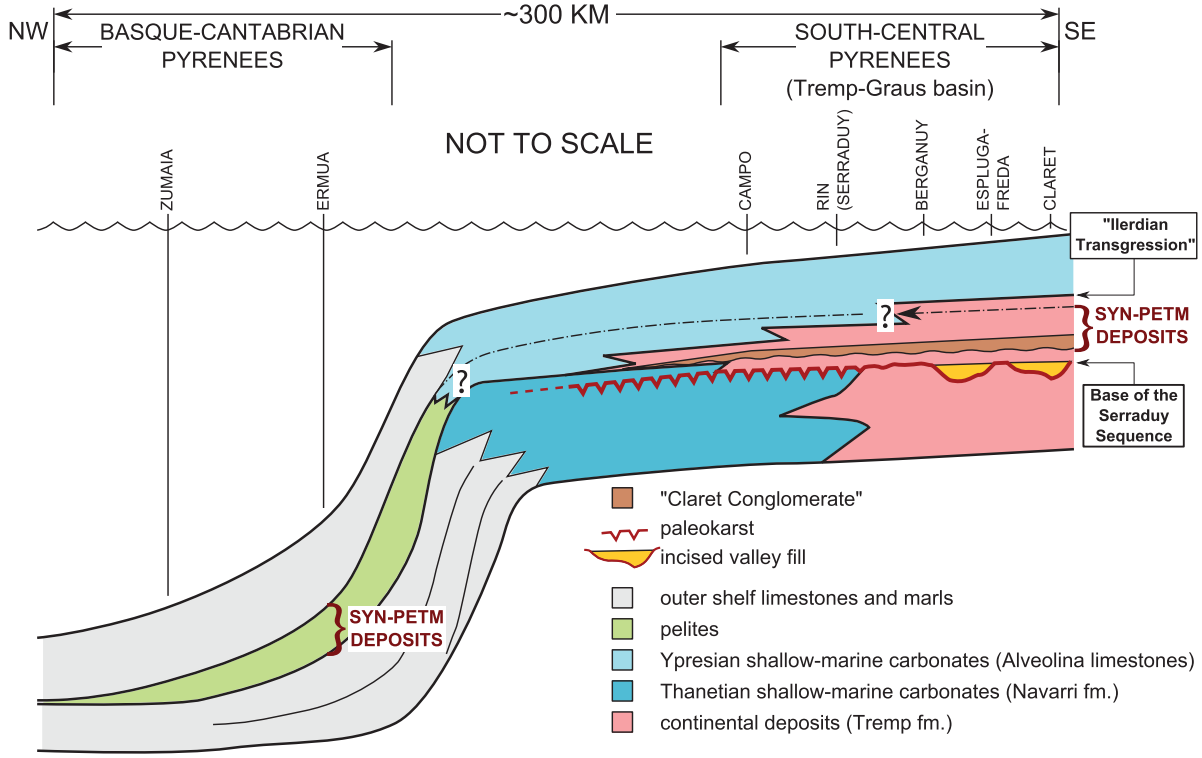

FIGURE 3 | Simplified reconstruction of an E-W transect in the southern Pyrenean foreland during the Ypresian (modified from Schmitz and Pujalte, 2003, after Schmitz and Pujalte, 2007; Baceta et al., 2011), displaying the location of the main Paleocene-Eocene thermal maximum sections, and the stratigraphic relationships of the thermal maximum with the units and surfaces discussed in the text. Notice that the range of this thermal maximum cannot be properly defined within the shallow-marine Ypresian carbonates (cf. Molina et al., 2003; Pujalte et al., 2009b), hampering a precise reconstruction of the lateral relationships between shallow and deep-marine deposits of the Basque-Cantabrian region in this specific interval.

was provided by Ullastre and Masriera (1998) in the eastern portion of the basin (Peralba section; Figs. 1C; 4). This section is very poorly exposed at present, particularly the finer-grained portions, and we have tentatively correlated our sections with it, since it is the only high-resolution record of the PETM interval in the Ager Basin available in the literature.

Facies analysis and stratigraphy

Facies analysis allowed to recognize 22 sedimentary facies (Table 1; Figs. 4; 5; 6) belonging to four main lithofacies: mudstones, carbonates, evaporites and siliciclastics. Sedimentary facies can be grouped into 9 facies associations representing 9 depositional elements and 5 continental to coastal and shallow-marine depositional systems (Table 2). The succession can be subdivided into 6 informal units (labeled A to F from the bottom; Fig. 4); each of them is a package of strata characterized by deposits formed in laterally related depositional systems. The surfaces separating these units (Fig. 4) represent abrupt facies changes (marking subaerial exposure and/or erosion and marine/lacustrine flooding surfaces). As a consequence, these units can represent systems tracts within depositional sequences developed on a decametric scale. Figure 4 displays the two logged sections and a possible correlation with the eastern Ager Basin.

Unit A

This unit is made up of continental deposits underlying the late Thanetian transgression (unit B); its base has been placed at the top (surface 0 – S0) of a 1m-thick paleosol horizon (last red soil (LRS), Figs. 1D, E; 4; facies m-r) representing a reliable local key horizon. Unit A is dominated by paleosols with variable degrees of maturity and/or humidity (mainly facies m-y and m-g; *cf.* Kraus and Riggins, 2007), and includes a lenticular body composed of lacustrine calcite-dominated carbonate deposits (facies m-l; Fig. 5A), and coastal saline lake deposits (facies e-m, e-l, e-n, e-d; Fig. 5B) enclosed within grey continental mudstones (facies m-g); thin organic matter-rich horizons (facies m-d) are also found in association with e-d dolomicrites.

Unit A pertains to the late transgressive portion of the Composite Thanetian sequence (CTS) of Rossi (1997a), and roughly overlaps with his small-scale depositional sequence 7. It is topped by a marine flooding surface (surface 1 – S1) placed at the first occurrence of marine fossils (oysters) within a package of grey mudstones (m-g/m-gb facies transition).This surface represents the base of the upper Thanetian marine carbonates of unit B.

Unit B

Unit B consists of marine deposits forming a ~25m-thick package of subtidal to intertidal fine-grained calcarenites (facies wa and rare gr-tb and gr-cl; Fig. 5C) and subordinate marls (facies m-gb). Vertical and lateral transitions (to the E) to peritidal micrites (facies mi-wa; Fig. 5D) are observed. This stratigraphic organization depicts an overall transgressive-regressive trend, as observed by Rossi (1997a).

The mi-wa deposits are topped in both sections by a paleokarst, locally expressed by a decimetric layer of micrite breccia (surface 2 – S2; Fig. 5D). Within the study area, the lateral continuity of the peritidal micrites just below S2 suggests a near-flat geometry for the paleokarst; we were not able to recognize this surface in the Peralba section, and the proposed correlation with Ullastre and Masriera's log (1998) is largely hypothetical.

Unit B roughly coincides with the small-scale sequence 8 of Rossi (1997a), and encompasses the maximum flooding to highstand stage of the CTS.

Unit C

Unit C is continuously exposed only in the Altera E section, where it is composed of a lower layer of yellow-mottled grey mudstones (facies m-g), and an upper yellow paleosol (facies m-y). The two are separated by a sharp surface, outlined by a thin micrite layer (facies mi-n; Fig. 5E). Centimetric yellowish-white carbonate nodules are also present above and below this surface. This is the only case of an evolved calcrete that we found in our study interval, possibly representing a Stage-IV calcrete (*sensu* Machette, 1985; *cf.* Alonso-Zarza and Wright, 2010). In the Altera W section, the mudstones of unit C are not exposed; however, a poorly-preserved, ~50cm-thick nodular gypsum layer (facies e-n) topped by a dolomicrite horizon (facies e-d), and an upper micrite layer (facies mi-l) have been observed, clearly indicating the occurrence of a relative base-level rise and the development of a small and isolated water body after the development of the S2 paleokarst.

This unit shows a variable thickness because of the erosional character of its upper boundary (surface 3 – S3); it is partially equivalent to the yellow to varicolored marls/mudstones unit in the Peralba section (Ullastre and Masriera, 1998); however, it is much thinner (~7m at Altera E, ~1m at Altera W and ~15m at Peralba). This suggests that the lower part of the yellow to varicolored marls/mudstones at Peralba (Fig. 4) could actually be a lateral equivalent of the regressive portion of unit B.

Unit C records the E-W transition from a supratidal coastal environment to an alluvial one; its aggradational stacking pattern indicates an accommodation space increase, related to a relative sea-level rise, following the phase of subaerial exposure and paleokarst development. This suggests that unit C may already belong to the transgressive system tract of the Serraduy Sequence.

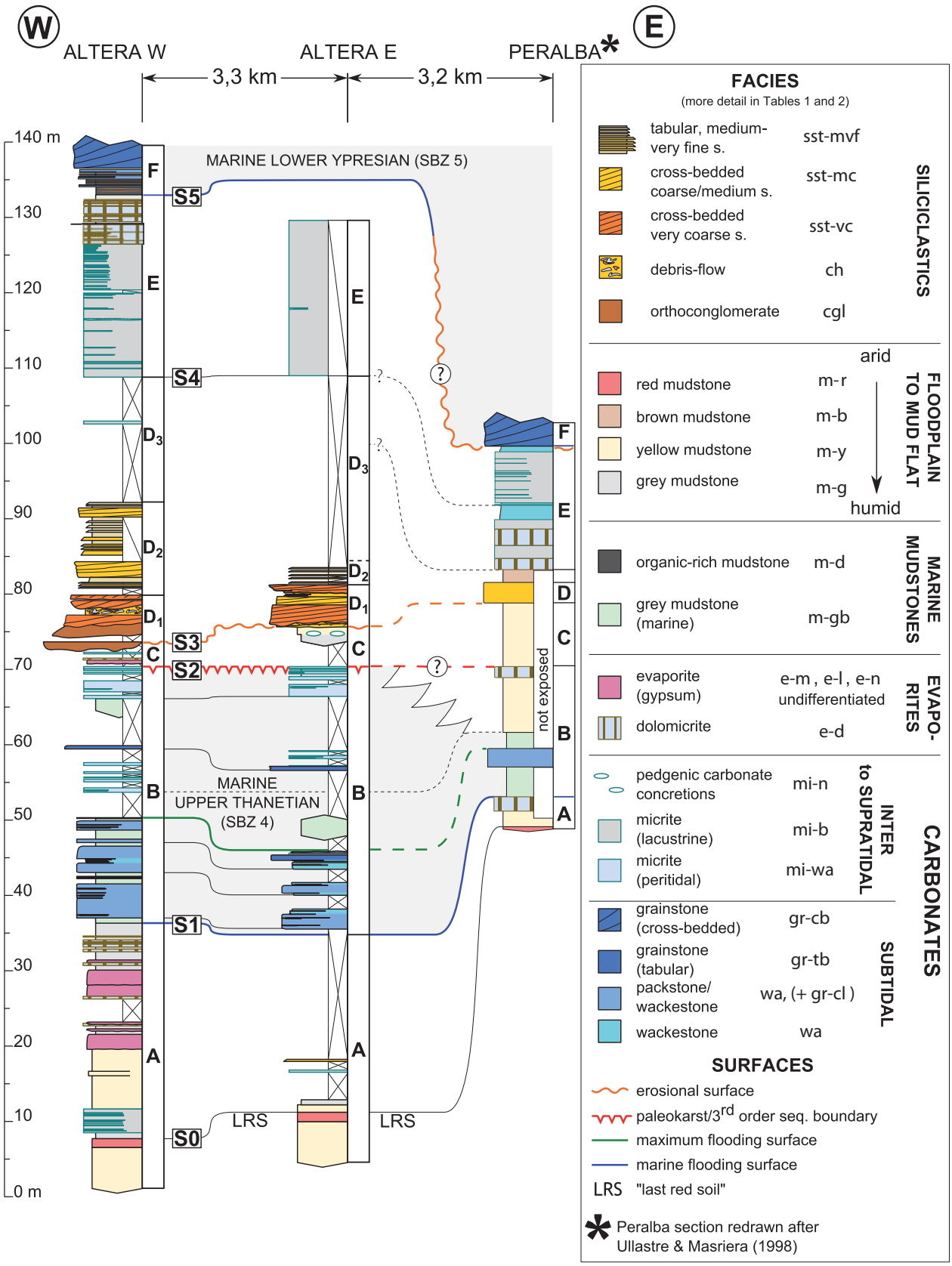

FIGURE 4 | Correlated stratigraphic logs of the studied sections, including a tentative correlation with the Peralba section from Ullastre and Masriera (1998); shaded areas represent the marine intervals.

TABLE 1 | Sedimentary facies recognized in the studied interval

Facies	Lithology	Interpretation
Mudstones		
m-r	red mudstones	well-drained, mature paleosol
m-b	brown mudstones	relatively mature paleosol
m-y	yellow mudstones	poorly drained, incipient paleosol
m-g	grey mudstones, locally yellow-mottled	mud flat/incipient paleosol
m-d	dark mudstones	swamp or lagoon
m-gb	grey-blue mudstones with marine fossils	lagoon/inner shelf
Carbonates		
mi-n	platy to nodular pedogenic micrite concretions	calcrete
mi-l	thin to medium-bedded micrites devoid of marine fossils	lacustrine calcitic deposits
mi-wa	laminated wackestones and micrites with miliolids	inter to supratidal deposits
gr-tb	massive, thin-bedded and relatively coarse-grained tabular grainstones	storm deposits?
gr-cl	poorly bioturbated calcarenites (fine-grained bimodal cross-laminated grainstones)	sand flat/mixed flat transition
wa	intensely bioturbated calcarenites (wackestones and wackestones/packstones)	inner shelf carbonates
gr-cb	large-scale cross-bedded coarse-grained grainstones with polymodal paleocurrents	bioclastic tidal bar
Evaporites		
e-m	grey mudstones with abundant gypsum nodules and veins	evaporitic mud flat
e-l	lenticular laminated gypsum	saline lake
e-n	nodular gypsum	early diagenetic product of facies e-l
e-d	dolomicrites, locally with gypsum molds	saline lake
Siliciclastics		
cgl	polymictic lenticular sandy orthoconglomerate with resedimented pedogenic detritus (paleosol nodules, Microcodium debris, peloids)	fluvial flood-related scouring and en-masse deposition (frictional freezing of the coarse head of a bipartite sediment-laden flow?) within a fluvial channel
ch	chaotic deposit with sandy matrix and abundant resedimented pedogenic (red mudstone clasts) and palustrine materials (oncoids, stromatolites, Microcodium debris, plant fragments)	frictional freezing of a debris flow conveyed in a fluvial channel
sst-vc	fan-shaped, scour-based, cross-bedded lenticular very coarse to medium-grained pebbly sandstones, with abundant mudstone clasts and plant fragments, sometimes bioturbated, high variability in paleocurrent directions	fluvial flood-related en-masse deposition, and partial winnowing within a channel or at its mouth during lower-regime fluvial activity
sst-mc	similar to sst-vc but medium to coarse-grained, with a less erosional or even transitional base (low-angle, thin-bedded bottomsets) and high-angle coarser foresets	mouth bar of a fluvial channel; minor erosion related with end of flow constriction
sst-mvf	medium to very fine-grained, tabular graded sandstones with planar to ripple- laminations and hummocky cross-stratifications, with abundant mudstone clasts and plant fragments, interbedded with siltstones-mudstones	unconfined fluvial flood deposits

Unit D

This unit has a basal erosional surface (S3) truncating unit C and consists of a ~35m-thick interval, organized in a ~20m-thick lower sandstone package (sub-units D1 and D2) and an upper, pelitic sub-unit (D3). The latter deposits are poorly exposed, with the exception of a few, very thin-bedded mi-l beds occasionally encountered in the Altera W section (this sub-unit may represent a transitional facies association between the siliciclastics of D1-D2 and the lacustrine carbonates of unit E). According to Ullastre and Masriera (1998), D3 sub unit can be correlated with the horizon of brown (facies m-b), continental marls of the Peralba section.

TABLE 2 | Facies associations and depositional systems recognized in the studied interval

Facies associations		Sedimentary environments	Depositional systems
FP	m-r, m-b, m-y, m-g, mi-n	floodplain	alluvial plain
FC	cgl, ch, sst-mvf	fluvial channel	
D	sst-mc, sst-mvf	frontal splay/delta	river delta?
CL	mi-l, m-g	carbonate lake (freshwater)	coastal lake
SL	e-m, e-n, e-l, e-d	salina lake	
MF	m-g, mi-wm	mud flat	inter to supra-tidal low-energy shoreline
CB	mi-wm, gr-cl, gr-tb	carbonate beach (peritidal)	
L	m-d, m-gb, wa, gr-tb	lagoon	shelf
S	gr-cb, gr-tb, m-gb	carbonate shelf	

The sandstone package is composed of coarse-grained, poorly sorted, lenticular and cross-bedded strata (facies sst-vc, sst-mc; Fig. 6A, B) and finer-grained, relatively better sorted tabular beds (facies sst-mvf; Fig. 6F). The lenticular sandstone bodies are mainly concentrated in the lower portion (sub-unit D1), where they are associated with basal massive or crudely cross-bedded orthoconglomerates (facies cgl, only occurring in the Altera W section; Fig. 6A, B, C), characterized by abundant reworked pedogenic material (reworked calcrete nodules and Microcodium debris). A chaotic deposit (facies ch; Fig. 6B) was found within sub-unit D1, similarly featuring abundant continental carbonate detritus (folded and convolute oncoids and stromatolitic matter), chunks of m-r paleosols squeezed between the more competent blocks, and a prevalently sandy matrix. This suggests deposition from subaerial debris flows, collecting detritus from both emerged areas (paleosols) and ponds (the carbonate material), and finally convoyed within fluvial channels.

In the Altera E section, the base of sub-unit D1 is represented by a couplet of cross-laminated sandstone beds, characterized by a large amount of mudstone clasts, truncated by large, coarse-grained cross-bedded sandstone bars (facies sst-mc with erosional base; Fig. 6D) with internal cross-laminations (mainly climbing dunes), large mudstone clasts and small wooden logs. The better exposed body shows internal scours in its upper portion, associated with a change in paleocurrents suggesting a local shallowing of the depositional profile. Each coarse-grained, cross-bedded body is apparently characterized by a different direction of accretion. In one dihedral exposure, bedding surfaces dip steeply to the south and more gently, with a slightly tangential basal contact, to the west, while internal cross-laminations are dominantly west-trending, apparently indicating a component of lateral accretion.

The finer-grained sub-unit D2 is entirely exposed only in the Altera W section, although fine-grained tabular beds can be encountered also to the east, indicating that the two sub-units are laterally continuous for at least some kilometers. In the Altera W section, these beds are represented by medium- to very fine-grained sandstones (facies sst-mvf; Fig. 6F). Moving slightly to the southeast from the section, a couple of small cross-bedded sandstone bars (facies sst-mc with transitional base; Fig. 6E) are present at two different levels, suggesting the occurrence of lateral facies transitions between the cross-bedded and tabular facies. This may be supported by the paleocurrent directions in the Altera W section, which display a general northern or north-western attitude.

We infer that facies sst-vc, sst-mc and sst-mvf represent a facies tract from fluvial channels to frontal splay (*sensu* Dreyer, 1993)/sheetflood deposits, altogether stacked in a backstepping pattern from D1 to D2. Facies sst-mc represents the transition from confined (facies sst-vc) to unconfined (facies sst-mvf) conditions, i.e a mouth-bar deposit. The scarcity of pedogenic features in the sst-mc deposits (only observed in the sub-unit D1 in the Altera E section), and their absence in the sst-mvf beds, may imply the occurrence of a relatively permanent water body to the north of the study locations, thus suggesting a deltaic origin of these deposits.

Apart from the aforementioned continental carbonate detritus (which is likely to represent coeval or slightly younger reworked material), the sandstones and conglomerates bear an abundant detrital carbonate component and a subordinate siliciclastic one (both quartz and lithic detritus), *i.e.* they are substantially similar in composition to the Thanetian fluvial sandstones of the Upper Tremp Fm. (*e.g.* Rossi, 1997b).

Unit D belongs to the Transgressive Systems Tract (TST) of the Serraduy sequence. We interpret the erosional features associated with sub-unit D1, rather than indicators of falling relative base-level, as related with the intensity of the flooding processes (see Discussion).

Unit E

Unit E is subdivided in two main packages of thin-bedded micrites, summing up for a total thickness of ~20m.

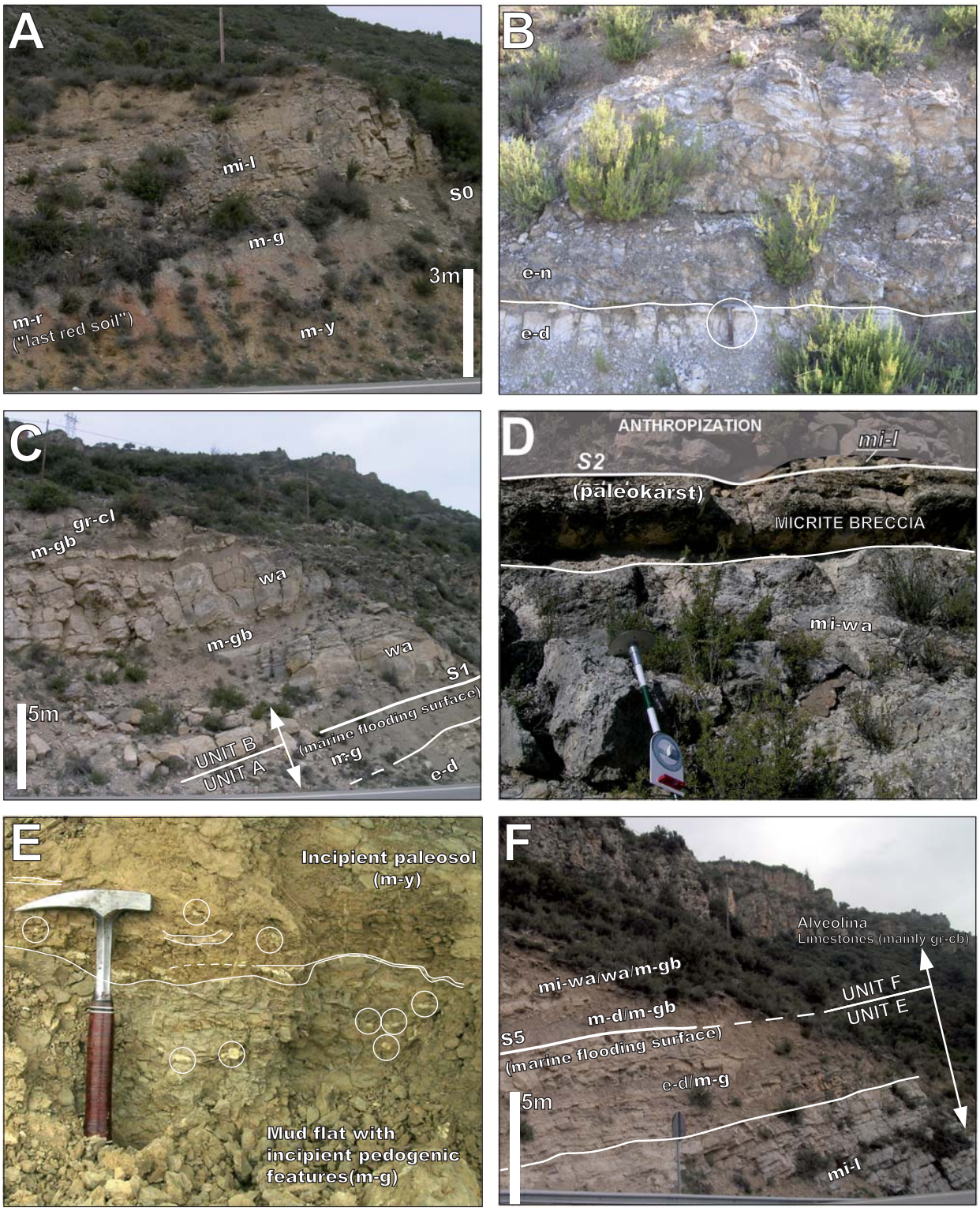

FIGURE 5 | Carbonate, mudstone and evaporitic facies recognized in the study area (see description in the text). A) Unit A (base of the studied interval), paleosols and lacustrine carbonates; B) Unit A, saline lake (evaporites and associated dolomicritic layer); C) Unit B, marine calcarenites; D) Unit B, peritidal micrites and paleo karst; E) Unit C, calcrete nodules (circled; facies mi-n); F) Units E and F, lacustrine to sabkha and marine deposits. Pictures A, B, C, F) Altera W section (C-13 roadcut); D, E) Altera E section. Hammer for scale in B and E is 33cm long; the Jacob Staff in d is subdivided in 10cm segments; rulers in A, C, F are referred to the foreground outcrop surface. m-r: red paleosols; m-y: yellow paleosol; m-g: grey paleosol; m-gb: marine mudstone; m-d: OM-rich mudstone; mi-l: lacustrine micrites; mi-wa: peritidal micrites; e-d: salina lake dolomicrite; e-n: salina-lake, nodular gypsum; wa: subtidal, fine-grained calcarenites; gr-cl: intertidal laminated calcarenites; gr-cb: bioclastic tidal bars.

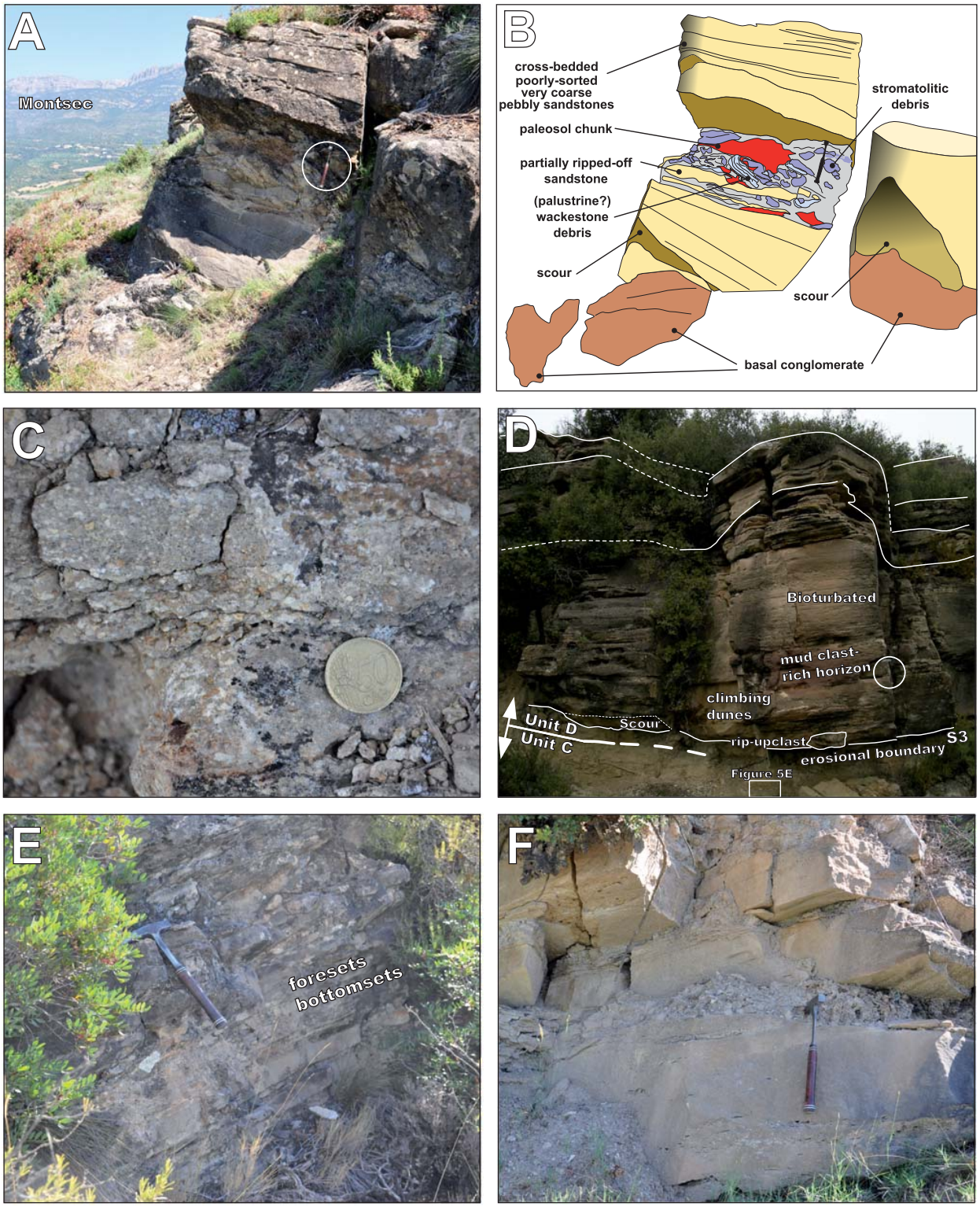

FIGURE 6 | Siliciclastic facies of unit D. A) Sub-unit D1, facies cgl (fluvial flood-related conglomerate deposit), ch (debris flow)and sst-vc (fluvial flood-related coarse-sandstones), view facing NW; B) interpretation of A; C) close-up view of facies cgl; D) Sub-unit D1, contact with unit C and different superposed sst-mc (mouth bar/frontal splay deposit) bodies, view facing N. E) Sub-unit D2, facies sst-mc, notice the coarsening upwards and the transitional contact at the base of the cross-bedded unit; F) facies sst-mvf (subaerial sheetflood deposits or delta-front lobes), fine-grained sheet sandstones (view facing NE). Pictures A, C, E, F) Altera W section. Hammer for scale in A, D, E, F is 33cm long, coin size is roughly 2cm diameter.

Its base is here designated as surface 4 (S4). Similar deposits typically underlie the Ypresian Alveolina Limestones in many locations of the southern Pyrenees (*cf.* Luterbacher, 1969; Mutti *et al.*, 1972), representing lacustrine/palustrine carbonate deposits. It is better exposed in the Altera W section (Fig. 5F), where it is organized in a lower, mainly micritic interval, with mi-l lenticular beds separated by very thin mudstone layers, and an upper, micritic-dolomitic interval with slightly thicker e-d deposits with thicker grey mudstone intercalations (facies m-g); small miliolids are occasionally found within the upper interval. Ullastre and Masriera (1998) reported the occurrence of wackestone layers with marine fossils and multiple dolomicritic intervals alternating in the lower portion in the eastern Ager Basin. This was not apparently the case for unit E in the Altera W exposure, but isotope data associated with mi-l carbonates could actually be related with fluctuating influences of marine and meteoric waters (see the Isotope data chapter).

Unit E represents the prosecution of a base-level rise trend initiated with unit C, thus it belongs to the TST of the Serraduy sequence.

Unit F

Fully-marine conditions are gradually re-established in the overlying unit F (Fig. 5F), composed of organic-rich m-d deposits, very rich in plant fragments and oysters, grading to grey mudstones interbedded with fine-grained shallow-water carbonates (facies m-gb, wa). The base of unit F is here designated as surface 5 (S5). For simplicity, we include in this unit the calcarenitic succession of the early Ypresian Alveolina Limestones, mainly composed of tide-dominated gr-cb deposits; in Figures 1D, F; S5 is approximated to the base of these deposits.

ISOTOPE DATA

Stable isotope analyses on carbonates were performed in order to constrain the location of the PETM CIE within the studied succession. This study was complicated by the poor outcrop conditions, the occurrence of lithological and environmental changes and diagenetic surfaces. Therefore, the results should be better considered as the isotope characterizations of distinct lithological units rather than long-term, climate-related variations.

Materials and Methods

Hand samples were collected from different stratigraphic levels in a variety of lithologies. Sub-samples were selectively extracted from fresh surfaces with a dentist drill, in order to verify if macroscopic internal heterogeneities of the samples (*e.g.* due to bioturbations, presence of Microcodium or color change) would be reflected in their isotope compositions. Marine calcarenites were instead treated as bulk.

38 sub-samples from 22 stratigraphic levels were prepared and analyzed at the Isotope Geochemistry Laboratory of the Parma University. The powders obtained from drilling were further grounded with an agate mortar, then weighed between 6.0 and 10.0mg for reaction with excess 100% phosphoric acid in a manually-operated vacuum line, at ~5*10-3atm and 25°C, for at least 12 hours.

Dolomite-bearing samples were treated with a two-steps procedure (Selmo, 1993) in order to separate the CO_2 evolved by calcite or dolomite reaction; they were weighed between 20.0 and 40.0mg and reacted in the same conditions. In this case, the CO_2 produced by the faster reaction of calcite was extracted after 2 hours for spectrometer analysis; the reaction was then continued for two more hours and further products of the reaction were removed. Finally, after at least 72 hours of reaction, the CO_2 freed from dolomite was extracted and analyzed separately. The analysis of CO_2 was performed with a Thermo Finnigan Delta S mass spectrometer by 8 comparisons with an internal standard (MAB99); all data are expressed in ‰ vs V-PDB. 25% of the sub-samples were double analyzed, with an analytical and instrumental error summing up to ±0.2‰.

Results

The diagrams of Figures 7 and 8 display the large field of $\delta^{13}C$ and $\delta^{18}O$ compositions represented by the analyzed samples; carbonates formed in a continental setting display a reduced variability in $\delta^{18}O$ values (ranging between -5‰ and -7‰) and a much wider range of $\delta^{13}C$ values; more complex distributions are observed in the marine and peritidal deposits. The stratigraphic calibration of these data allows a better understanding of the isotope signatures and shifts (Fig. 9). In general, we consider the carbon isotope ratio more reliable in terms of preservation than the oxygen one (*cf.* Marshall, 1992).

Dolomicrite (facies e-d; unit A and top of unit E)

These deposits were recognized at the base and top of the studied succession in the Altera W section. Their $\delta^{13}C$ composition ranges from -0.5‰ to 1‰ for calcite and from 0‰ and 1.2‰ for dolomite (dolomite $\delta^{13}C$ is always more negative than calcite $\delta^{13}C$, of a -0.5‰). Dolomicrites from unit A display a slightly heavier carbon composition (by a 1‰).

Marine calcarenite (facies wa, gr-tb; unit B)

These calcarenites display a sharp signature with $\delta^{18}O$ more negative than $\delta^{13}C$. The role of diagenetic secondary

calcite is probably significant because of the high porosity of these rocks. Bulk $\delta^{13}C$ ranges between -1‰ and 3‰, and is comparable to similar coeval deposits (*cf.* Zamagni *et al.*, 2012).

Peritidal micrites (facies mi-wa; unit B)

The isotope composition of these micrites shifts considerably, from slightly positive values to negative values while approaching the S2 paleokarst. This is a typical diagenetic imprint, clearly related with the exposure surface (*cf.* Immenhauser *et al.*, 2002, with references therein). Peak negative values for $\delta^{13}C$ overlap with the field of Thanetian lacustrine carbonates (roughly across -4‰).

Pedogenic carbonate concretions (facies mi-n; unit C)

These concretions display a negative signal in $\delta^{13}C$ and $\delta^{18}O$, consistent with a pedogenic origin. The $\delta^{13}C$ ranges across -8‰, consistent with non-PETM values from comparable samples in the Tremp-Graus Basin (Schmitz and Pujalte, 2003, 2007).

Carbonate clasts of unit D (carbonate nodules within facies cgl)

Different carbonate clasts from the basal conglomerate of unit D in the Altera W section were sampled for isotope analyses (white, yellow and pink micrite clasts). Their isotope compositions are plotted in detail in the diagram of Figure 8. Yellow clasts display peak negative $\delta^{13}C$ values, but this could be possibly due to recent weathering. White and pink clasts, apparently unaltered, still display a very negative signal (ranging across -12‰), consistent with the syn-PETM values for soil nodules recorded in the Tremp-Graus Basin (Schmitz and Pujalte, 2003).

Lacustrine (calcitic) carbonate (facies mi-l; units A, C, D and E)

Lacustrine micrites display a significant variability in isotope compositions. However, the values recorded in unit A and D-E are rather clustered in two distinct fields, with an average -3‰ lighter $\delta^{13}C$ composition for the samples of unit E. This unit also displays the major internal variability, which ranges from -9 to -6‰ (average: -7.33‰, standard deviation 0.79); at least part of this variability may be related to a contribution of marine waters. Within this range are also included a thin lacustrine layer located just below S3 (roughly -6‰) and a stromatolite clast (roughly -7‰) from the debris flow of sub-unit D1 in the Altera W section.

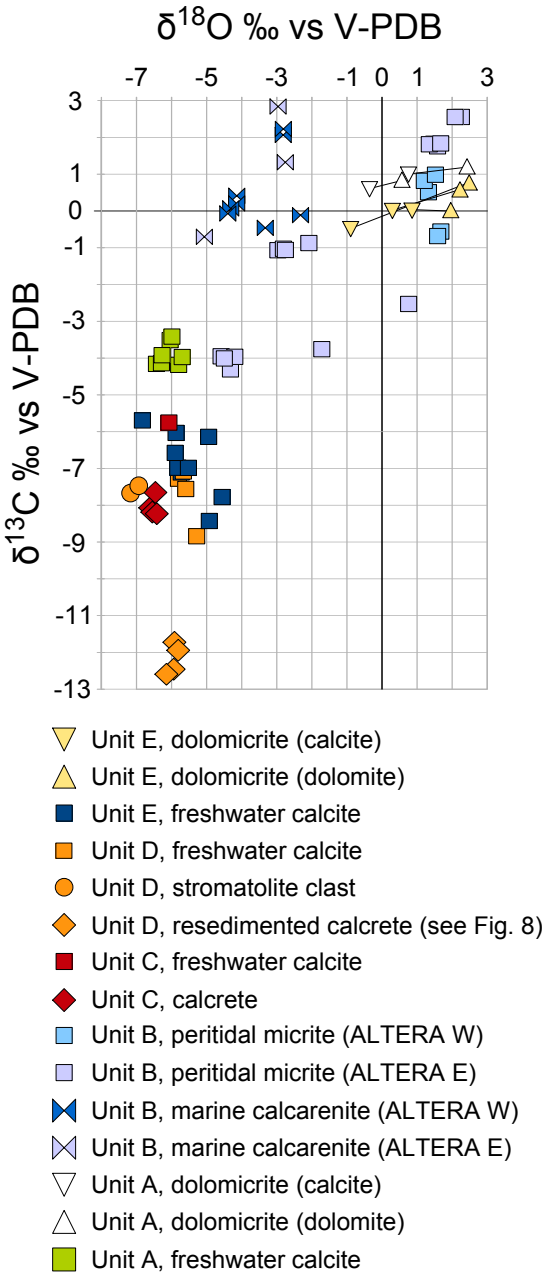

FIGURE 7 | Stable isotope composition of the carbonate deposits in the study area (see text for description).

DISCUSSION

The Paleocene-Eocene thermal maximum in the Ager Basin: isotope evidence

Multiple evidences, both from the peri-Pyrenean realm and at global scale (*e.g.* Gibson *et al.*, 2000; Schmitz and Pujalte, 2003; Bowen *et al.*, 2004) indicate the occurrence during the PETM of humid, or seasonally humid climate which enhanced land erosion and continental runoff. The case of the southern Central Pyrenees foreland basin

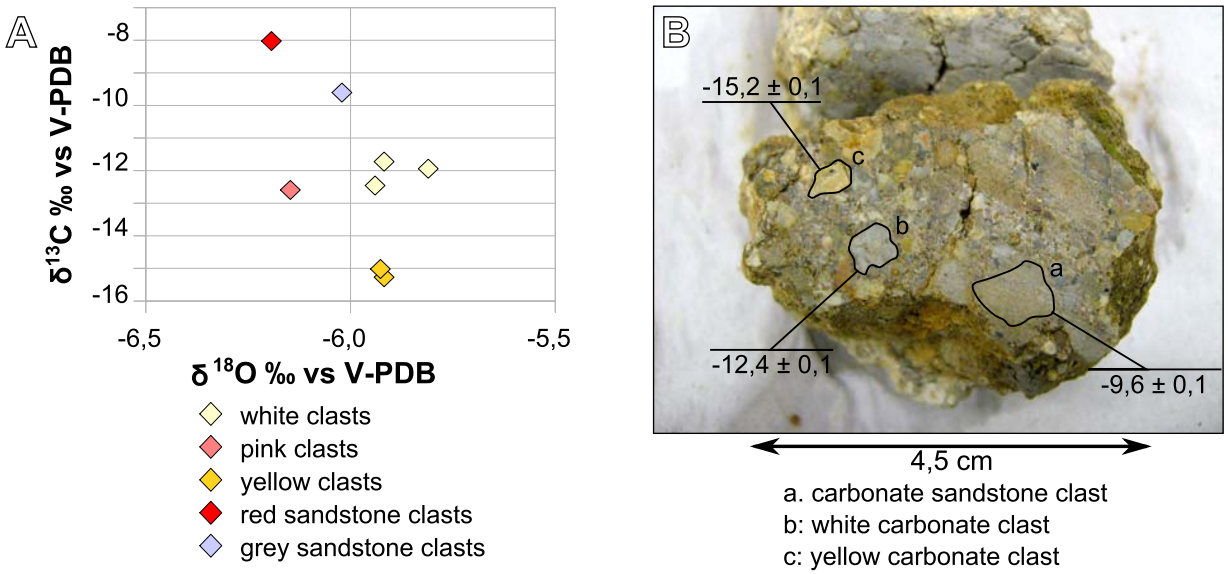

FIGURE 8 | A) stable isotope compositions of the resedimented carbonates from the basal conglomerate of unit D in the Altera W section; B) detail of hand sample.

is characterized by a contrast between these transient conditions and the overall Paleocene arid climate.

In the Ager Basin, within the biostratigraphically-constrained Paleocene-Eocene boundary interval (units C, D, E), fluvial systems (unit D) set up abruptly along a coastline dominated by tidal flat and sabkha environments. The isotope profile in Figure 9 depicts an apparent negative isotope excursion (-8‰) in the Altera W section, roughly between 70 and 120m, in large part related with the shift from marine to continental deposits, thus the occurrence of the PETM CIE may be difficult to constrain. In Figure 10 we isolated the $\delta^{13}C$ values of samples with a similar facies from within and outside the Paleocene-Eocene boundary interval. The largest CIE (roughly -4‰) occurs between the in place carbonate concretions within unit C and the resedimented ones within the basal conglomerate of unit D. The negative peak $\delta^{13}C$ (less than -11‰ vs V-PDB) is in agreement with syn-PETM values in carbonate soil nodules from the Tremp-Graus Basin (Fig. 11; Schmitz and Pujalte, 2003; Schmitz and Pujalte, 2007). A similar shift (roughly -3‰), although on different background values, occurs between the Thanetian lacustrine micrites from unit A and the ones from the top of unit D and the lower portion of unit E. On the other hand, dolomicrites from the Thanetian and from the top of the Paleocene-Eocene boundary interval display substantially comparable $\delta^{13}C$ values.

We interpret unit D as a suite of deposits that are coeval with the PETM. Our data, however, do not allow us to properly locate the PETM onset; we also speculate that this event could have been recorded in an uppermost part, here eroded below S3, of unit C, rather than being definitely coeval with the base of the fluvial systems of unit D. Despite this problem, the unconformity at the base of unit D represents a good approximation for the Paleocene-Eocene boundary, especially for mapping purposes. According to our correlation, this erosion may have been relatively moderate (a few m in the Altera W section) and localized in small channel incisions; nevertheless, there may still be a chance for the preservation of the actual Paleocene-Eocene boundary, since a carbonate layer just below S3 in the Altera W section displays $\delta^{13}C$ values comparable to the ones of unit E (thus the actual Paleocene-Eocene boundary may be contained within unit C). We propose that the problem could be worked out through $\delta^{13}C$ analysis of the organic matter of unit C, in order to obtain data from those portions devoid of primary carbonate precipitates.

Although we spotted a PETM-consistent CIE also between the lacustrine deposits of units A and E (Fig. 10), the interpretation of unit E's isotope values is more problematic because of their greater vertical variability, possibly related to episodic variations of water composition (*e.g.* a marine influx in the lacustrine body). A similar situation may occur in the outer Tremp-Graus Basin (Campo section; Pujalte *et al.*, 2009a, fig. 4). In this section, a continental carbonate layer (palustrine limestone) is interposed between a paleosol overlying the local equivalent of the Claret Conglomerate and the first marine Ypresian beds. This layer apparently represented a post-PETM horizon, with $\delta^{13}C$ values ranging around -6‰ (whereas the $\delta^{13}C$ value in the underlying paleosol is roughly -9‰). The change of lithology probably forced the authors to discard the possibility to interpret this shift as a PETM recovery trend, which is thought to occur here after the marine ingression

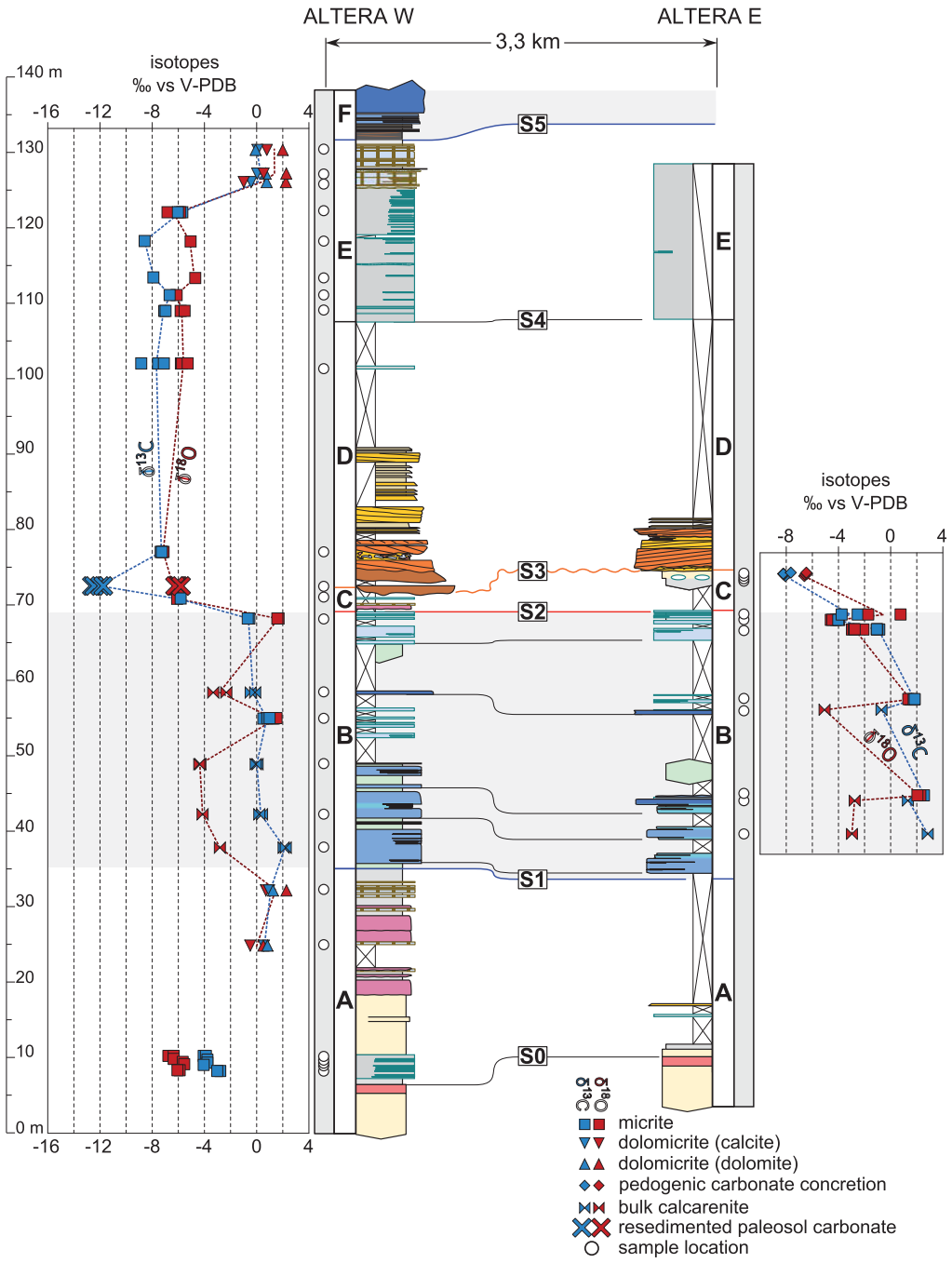

FIGURE 9 | Vertical variability of the stable isotope data compared with the stratigraphic succession (compare with Fig. 7).

(*cf.* Pujalte *et al.*, 2009b). As we hypothesized for Ager Basin's unit E, the $\delta^{13}C$ values for palustrine carbonates in the Campo section could then reflect syn-PETM values for carbonates formed in environments characterized by a mixture of meteoric and marine waters .

Finally, since the $\delta^{13}C$ of the dolomicritic deposits on top of unit E are poorly scattered from their Thanetian equivalents, we infer that non-PETM conditions are restored at this point.

The Paleocene-Eocene thermal maximum in the Ager and Tremp-Graus basins: physical-stratigraphic implications

In Figure 11 we summarized the main aspects of the PETM record in the Ager Basin and inner Tremp-Graus Basin and its relationships with sedimentological and sequence-stratigraphic features.

Ager Basin's unit D formed upon coastal deposits and incipient paleosols (unit C), which represent a period of

relative base-level rise following a more or less prolonged lowstand recorded by the S2 paleokarst. Following Rossi (1997a), we attributed a regional significance to this surface, equivalent to the basal boundary of the Serraduy sequence of Luterbacher *et al.* (1991). Moderate erosion affected unit C at the onset of the fluvial systems (S3); also, the lower portion of unit D (sub-unit D1) displays a number of internal erosional surfaces, thus it was clearly formed under conditions of low rates of creation of accommodation space, and consequent flow constriction; these conditions could indicate that the deposition of unit D followed an episode of relative sea-level fall; similar conditions were also considered by Schmitz and Pujalte (2003), concerning the initial PETM in the Tremp-Graus Basin. Despite some arguments for rising/falling global sea-level during the PETM (*e.g.* Sluijs *et al.*, 2011, with references therein), the southern Central Pyrenees foreland basin may be affected by different forcings, since relative sea-level variations in a foreland basin can be significantly influenced by its tectonic evolution. As an example, the occurrence of a marine upper Thanetian and a thick lacustrine body across the Paleocene-Eocene boundary interval throughout the southern Ager Basin (absent in the inner Tremp-Graus Basin) is probably related with the structural control, *i.e.* the depositional profile of the basin was slightly lowered with respect to the inner portion of the Tremp-Graus Basin, due to the load of the Montsec thrust

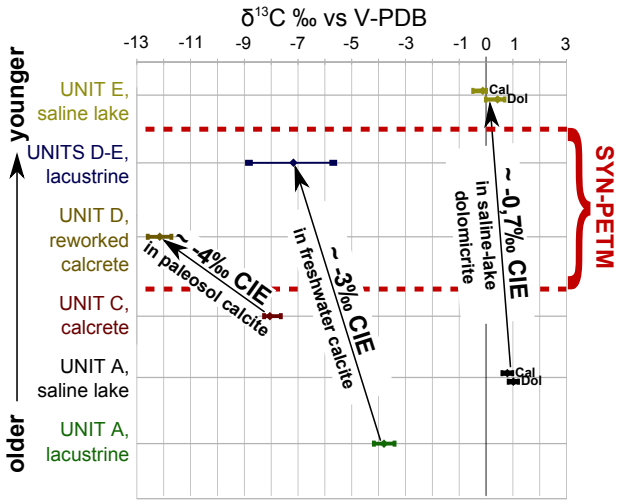

FIGURE 10 | Synthesis of the $\delta^{13}C$ composition of three main carbonate facies (calcretes, lacustrine carbonates and saline lake dolomicrites) across the P/E boundary interval, indicating the occurrence of a consistent isotope perturbation in the inorganic carbon pool at the time of the formation of unit D and the lacustrine/calcitic portion of unit E. Dolomicrites from saline lake environments (unit A and top of unit D) do not bear the signs of a similar perturbation. By considering the stratigraphic order of the samples (left), and their relationships with biozones (cf. Fig. 2; 6), these data apparently constrain the occurrence of the Carbon Isotope Excursion of the Paleocene-Eocene Thermal Maximum (PETM CIE) (right); the onset may occur within an unsampled layer of unit C, or it may have been eroded at the base of unit D (S3).

sheet (an alternative explanation, or a concurring factor, may be represented by higher sedimentation rates in the flood-plains of the Tremp-Graus Basin, related with the proximity of the incipient Pyrenean orogen to the north).

As evidenced by Mutti *et al.* (1996), Mutti *et al.* (2000) and Mutti *et al.* (2003), the role of fluvial floods may be a critical issue in the interpretation of the stratigraphic framework of foreland basins, where strong topographic gradients provide both a larger surface available for erosion, and the conditions to form small fluvial systems (*sensu* Milliman and Syvitsky, 1992) dominated by episodic floods.

We propose that a consistent, short-term increase in fluvial discharge, triggered by a climatic forcing, may produce, in a coastal environment, stratigraphic features similar to sequence boundaries and lowstand systems tracts, at regional or global scales (such as the case for the PETM climatic anomaly): stillstand or even rising base levels may not keep up with sedimentation, especially when subsidence rate is slow, so that shallowing-upwards trends, not driven by eustasy or subsidence, occur; when the fluvial activity reaches its peak with catastrophic floods, erosional features, avulsion and compensational geometries may develop both in the floodplain and at the mouth of fluvial channels. An example of this process is represented by the deep scouring in the terminal portion of fan-deltas, operated by highly energetic and sediment-laden fluvial floods, indicated as the process behind the formation of the flood-dominated sigmoidal mouth bars of Mutti *et al.* (1996). This kind of depositional element may represent an alternative interpretation for the channelized deposits of Sub-unit D1 in the Altera W section; however, the correct recognition of this facies would require better exposures than the ones available.

The backstepping pattern recorded in sub-unit D2, interpreted as a vertical transition to unconfined, possibly deltaic or sheetflood systems, indicates a turning point in the balance between climate-driven sediment discharge and base-level rise. We suggest that a decrease in land-erosion and discharge with the consequent lower sediment input to the basin could be more significant, rather than an acceleration in base-level rise.

The coarser-grained clastic deposits associated with the earliest stages of the PETM and the occurrence of debris flows could represent the catastrophic impact of a twisted climatic regime over a landscape in equilibrium with arid conditions. A few tens of kiloyears after the onset of the thermal maximum may represent a sufficient time lag for re-equilibrating the depositional profile to the new regime, after the deflation of most of the loose or more erodible materials available before the thermal maximum. This

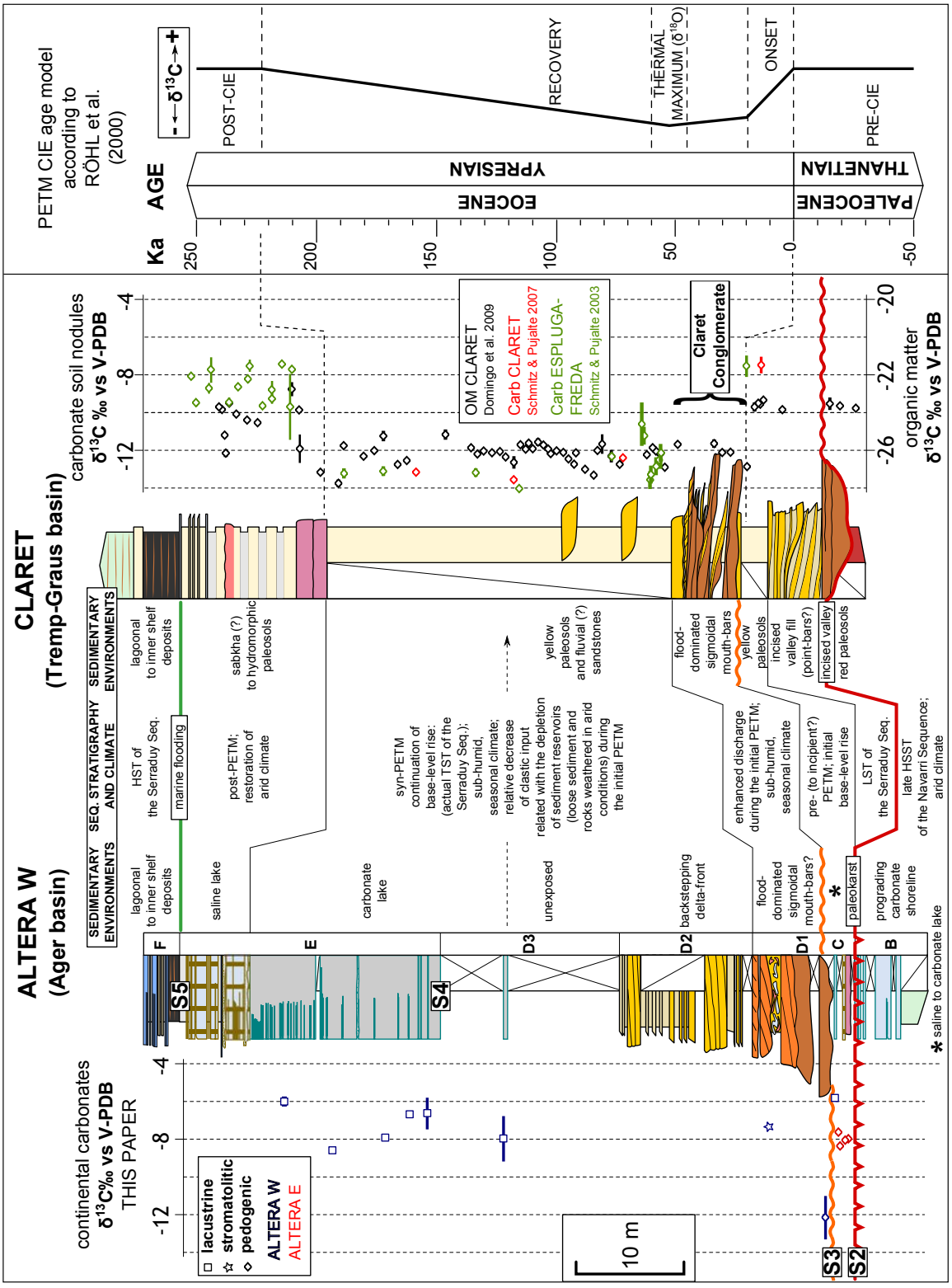

FIGURE 11 Representative logs of the lower part of the Serraduy sequence in the Ager and Tremp-Graus basins. S2 corresponds to the lower sequence boundary; according to Pujalte et al. (2009b), the transgressive surface of the Serraduy sequence (onset of the Ilerdian transgression) should be closely related with the onset of the Paleocene-Eocene Thermal Maximum (PETM). In the Ager Basin, the sequence boundary and the transgressive surface are coincident. The Claret conglomerate (facies interpretation following Mutti, 2008) and its Ager equivalent (sub-unit D1) are related to an event of enhanced sediment supply and, for cartographic purposes, their base is an optimal approximation for the onset of the PETM, i.e. for the P/E boundary. Isotope data from the Esplugafreda section have been included since they represent the most complete PETM carbonate record in the southern Central Pyrenees foreland basin; the data interval was matched to the correlative units in the Claret section (syn-PETM yellow paleosols; post-PETM evaporites). OM-carbon data from Domingo et al. (2009) provide a more complete PETM record. Discussion in the text.

would cause a relative reduction in sediment handled by rivers during the later stages of the PETM.

This stratigraphic pattern may be recognized as well in the syn-PETM interval in the northern Tremp-Graus Basin (we specifically refer to the organic-matter $\delta^{13}C$ record provided by Domingo *et al.* (2009) in the Claret and Tendruy sections, which represents a more continuous dataset than the one based on paleosol nodules). The early stages of the CIE are associated with widespread, laterally continuous, very coarse-grained and relatively thin-bedded alluvial deposits, the Claret Conglomerate, characterized by basal and internal scours and marked progradational geometries; during the main body of the CIE, instead, the succession is dominated by muddy/silty deposits with relatively immature paleosols, hosting a few minor siliciclastic bodies. Pujalte *et al.* (2009b), in a general overview of the Paleocene-Eocene boundary in the South-Pyrenean foreland, demonstrated that this interval (coarse clastics + yellow paleosols) formed during overall transgressive conditions (Ilerdian transgression; *cf.* Fig. 3). We interpret that, the Yellow paleosols and their marine equivalents could correlate with the interval including sub-units D2-D3 and the lacustrine portion of unit E.

The apparent recovery from the CIE that we recorded at the top of unit E, concurrent with a change from lacustrine to evaporitic deposits, has a good analog in the inner Tremp-Graus Basin, with the development of an evaporitic setting at the end of the PETM and just before the Ilerdian marine flooding.

CONCLUSIONS

The Paleocene-Eocene boundary in the Baronia Trough of the southern Ager Basin was constrained to a very narrow interval on the basis of a -4‰ CIE between in situ and fluvial resedimented paleosol nodules, indicating that the onset of the PETM (global standard for the Paleocene-Eocene boundary) is coeval with (or possibly slightly younger than) the erosional base of a fluvial sandstone unit (surface 3, unit D).

The stratigraphic record of the PETM was tentatively defined by comparing isotope data from different Thanethian carbonate deposits and from deposits pertaining to the Paleocene-Eocene boundary interval (units C, D, E) in the southern Ager Basin; our interpretation is supported by strong similarities with the litho- and sequence-stratigraphy record of the PETM in the Tremp-Graus Basin.

We discussed the stratigraphic and sedimentological effects of the PETM in the southern Central Pyrenees foreland basin, starting from the considerations of Schmitz and Pujalte (2003, 2007). We propose a model to explain the occurrence of fluvial and fluvio-deltaic sandstones coeval with the supposed early stages of the PETM (and apparently representing a local sequence boundary), and the gradual reduction of fluvial discharge during the main body of the isotope excursion, as the effect of a major availability of loose sediment at the time the climate anomaly broke through. This increased sediment input produced a regressive pattern competing with, and initially taking over, an overall sea-level rise, which may have been coeval with the entire thermal maximum. This framework could be a specific issue of the southern Central Pyrenees foreland basin, with relative sea-level trends influenced by local subsidence patterns, and should not be generalized.

If our conclusions on the stratigraphic range of the PETM in the Ager Basin are correct, we could better constrain also the age of the Ilerdian marine flooding (base of unit F) which, in the Baronia Trough, is older than in the outer Tremp-Graus Basin (Campo section) and substantially coeval, or perhaps slightly younger than in the inner Tremp-Graus Basin (Claret section).

ACKNOWLEDGMENTS

We would like to thank E. Mutti for having introduced us to the geology of the southern Central Pyrenees foreland basin, and his original suggestion of an equivalence between the siliciclastic deposits of the Paleocene-Eocene boundary interval in the Ager Basin and the Claret conglomerate of the Tremp-Graus Basin. We also thank R. Tinterri for his support and suggestions. G. Villa for supporting our work and E.M. Selmo for helping out in the interpretation of the dolomite/calcite isotope data and for general support at the Isotope Geochemistry Laboratory at the Physics and Earth Sciences Department of the Parma University.

REFERENCES

Alonso-Zarza, A.M., Wright, V.P., 2010. Calcretes. In: Alonso-Zarza, A.M., Tanner, L.H. (eds.). Carbonates in continental settings: facies, environments and processes. Oxford, Elsevier, 225-267.

Aubry, M.P., Ouda, K., Dupuis, C., Berggren, W.A., Van Couvering, J.A., Ali, J.R., Brinkhuis, H., Gingerich, P.R., Heilmann-Clausen, C., Hooker, J., Kent, D.V., King, C., Knox, R.W.O'B., Laga, P., Molina, E., Schmitz, B., Steurbaut, E., Ward, D.R., 2007. The Global Standard Stratotype-section and Point (GSSP) for the base of the Eocene Series in the Dababiya section (Egypt). Episodes, 30(4), 271-286.

Baceta, J.I., Pujalte, V., Bernaola, G., 2005. Paleocene coralgal reefs of the western Pyrenean basin, Northern Spain: New evidence supporting an earliest Paleogene recovery of reefal ecosystems. Palaeogeography, Palaeoclimatology, Palaeoecology, 224, 117-143.

Baceta, J.I., Pujalte, V., Wright, V.P., Schmitz, B., 2011. Carbonate platform models, sea-level changes and extreme climatic events during the Paleocene/early Eocene greenhouse interval. In: Arenas, C., Pomar, L., Colombo, F. (eds.). Pre-Meeting Field trips Guidebook. Zaragoza, 28th IAS Meeting, Geo-Guías 7, Sociedad Geológica de España, 101-150.

Barberà, X., Marzo, M., Reguant, S., Samsó, J.M., Serra-Kiel, J., Tosquella, J., 1997. Estratigrafía del grupo Fígols (Paléogeno, Cuenca de Graus-Tremp, NE de España). Revista de la Sociedad Geológica de España, 10(1-2), 67-81.

Bowen, G.J., Beerling, D.J., Koch, P.L., Zachos, J.C., Quattlebaum, T., 2004. A humid climate state during the Palaeocene/Eocene thermal maximum. Nature, 432, 495-499.

Colombo, F., Cuevas, J.L., 1993. Características estratigráficas y sedimentológicas del Garumniense en el sector de Ager (Pre-Pirineo, Lleida). Acta Geologica Hispanica, 28(4), 15-32.

Crouch, E.M., Heilmann-Clausen, C., Brinkhuis, H., Morgans, H., Rogers, K.M., Egger, H., Schmitz, B., 2001. Global dinoflagellate event associated with the late Paleocene thermal maximum. Geology, 29, 315-318.

Dickens, G.R., O'Neil, J.R., Rea, D.K., Owen, R.M., 1995. Dissociation of oceanic methane hydrate as a cause of the carbon isotope excursion at the end of the Paleocene. Paleoceanography, 10(6), 965-971.

Domingo, L., López-Martínez, N., Leng, M.J., Grimes, S.T., 2009. The Paleocene-Eocene Thermal Maximum record in the organic matter of the Claret and Tendruy continental sections (South-Central Pyrenees, Lleida, Spain). Earth and Planetary Science Letters, 281, 226-237.

Dreyer, T., 1993. Quantified fluvial architecture in ephemeral stream deposits of the Esplugafreda Formation (Palaeocene), Tremp-Graus Basin, northern Spain. In: Marzo, M., Puigdefábregas, C. (eds.). Alluvial sedimentation. Special Publication of the International Association of Sedimentologists, 17, 337-362.

Eichenseer, H., Luterbacher, H.P., 1992. The Marine Paleogene of the Tremp region (NE Spain). Depositional sequences, facies history, biostratigraphy and controlling factors. Facies, 27, 119-152.

Feist, M., Colombo, F., 1983. Le limite Crétace-Tertiaire dans le nord-est de l'Espagne du point de vue des charophytes. Géologie Méditerraneenne, 10, 303-325.

Ferrer, J., Le Calvez, Y., Luterbacher, H.P., Premoli-Silva, I., 1973. Contribution à l'étude des foraminiféres ilerdiens de la région de Tremp (Catalogne). Mémoires du Muséum National de Histoire Naturelle, Sciences de la Terre, 29.

Galbrun, B., Feist, M., Colombo, F., Rocchia, R., Tambareau, Y., 1993. Magnetostratigraphy and biostratigraphy of Cretaceous-Tertiary continental deposits, Ager basin, Province of Lerida, Spain. Paleogeography, Palaeoclimatology, Palaeoecology, 102, 41-52.

Gibson, T.G., Bybell, L.M., Mason, D.B., 2000. Stratigraphic and climatic implications of clay mineral changes around the Paleocene/Eocene boundary of the northeastern US margin. Sedimentary Geology, 134(1-2), 65-92.

Gradstein, F.M., Cooper, R.A., Sadler, P.M., Hinnov, L.A., Smith, A.G., Ogg, J.G., Villeneuve, M., McArthur, J.M., Howarth, R.J., Agterberg, F.P., Robb, L.J., Knoll, A.H., Plumb, K.A., Shields, G.A., Strauus, H., Veizer, J., Bleeker, W., Shergold, J.H., Melchin, M.J., House, M.R., Davydov, V., Wardlaw, B.R., Luterbacher, H.P., Ali, J.R., Brinkhuis, H., Hooker, J.J., Monechi, S., Powell, J., Röhl, U., Sanfilippo, A., Schmitz, B., Lourens, L., Hilgen, F., Shackleton, N.J., Laskar, J., Wilson, D., Gibbard, P., Van Kolfschten, T., 2004. A Geological Time Scale 2004. Cambridge University press, 589pp.

Immenhauser, A., Kenter, J.A.M., Ganssen, G., Bahamonde, J.R., Van Vliet, A., Saher, M.H., 2002. Origin and significance of isotope shifts in Pennsylvanian carbonates (Asturias, NW Spain). Journal of Sedimentary Research, 72(1), 82-94.

Institut Cartogràfic de Catalunya, 2003. Mapa geològic de Catalunya 1:250.000, 1 map.

Kennett, J.P., Stott, L.D., 1991. Abrupt deep-sea warming, palaeoceanographic changes and benthic extinctions at the end of the Palaeocene. Nature, 353, 225-229.

Koch, P.L., Zachos, J.C., Gingerich, P.D., 1992. Correlation between isotope records in marine and continental carbon reservoirs near the Palaeocene/Eocene boundary. Nature, 358, 319-322.

Kraus, M.J., Riggins, S., 2007. Transient drying during the Paleocene-Eocene Thermal Maximum (PETM): Analysis of paleosols in the Bighorn basin, Wyoming. Palaeogeography, Palaeoclimatology, Palaeoecology, 245, 444-461.

López-Martínez, N., Arribas, M.E., Robador, A., Vicens, E., Ardévol, L., 2006. Los carbonatos danienses (Unidad 3) de la Fm. Tremp (Pirineos Sur-Centrales): paleogeografía y relación con el límite Cretácico-Terciario. Revista de la Sociedad Geológica de España, 19(3-4), 233-255.

Luterbacher, H.P., 1969. Remarques sur la position stratigraphique de la formation d'Ager (Pyrenées Méridionales). Bulletin du Bureau de Recherches Géologiques et Minières, 69, 225-232.

Luterbacher, H.P., Eichenseer, H., Betzler, C., Van Den Hurk, A.M., 1991. Carbonate-siliciclastic depositional systems in the Paleogene of the South-Pyrenean foreland basin: a sequence-stratigraphic approach. In: Macdonald, D.I.M. (ed.). Sedimentation, tectonics and Eustasy: Sea-Level Changes at Active Margins. Special Publication of the International Association of Sedimentologists, 12, 391-407.

Machette, M.N., 1985. Calcic soils of southwestern United States. In: Weide, D.L. (ed.). Soil and quaternary Geology of the southwestern United States. Special Paper of the Geological Society of America, 203, 1-21.

Marshall, J.D., 1992. Climatic and oceanographic isotopic signals from the carbonate rock record and their preservation. Geological Magazine, 129(2), 143-160.

Mey, P.H.W., Nagtegaal, P.J.C., Roberti, K.J., Hartevelt, J.J.A., 1968. Lithostratigraphic subdivision of Post-hercinian deposits in the south-central Pyrénées, Spain. Leidse Geologische Mededelingen, 41, 21-228.

Milliman, J.D., Syvitsky, J.P.M., 1992. Geomorphic/Tectonic Control of Sediment Discharge to the Ocean: The Importance

of Small Montainous Rivers. Journal of Geology, 100(5), 525-544.

Minelli, N., 2012. Integrated Stratigraphy of the upper Paleocene-lower Eocene successions of the Tremp and Ager basins (south-central Pyrenees, Spain). Doctoral Thesis. Parma, Università degli Studi di Parma, 244pp.

Molina, E., Angori, E., Arenillas, I., Brinkhuis, H., Crouch, E.M., Luterbacher, H.P., Monechi, S., Schmitz, B., 2003. Correlation between the Paleocene/Eocene boundary and the Ilerdian at Campo, Spain. Revue de micropaléontologie, 46, 95-109.

Muñoz, A., 2002. The Pyrenees. In: Gibbons, W., Moreno, M.T. (eds.). The Geology of Spain. London, Geological Society, 370-385.

Mutti, E., 2008. Facies interpretation of the Claret Conglomerate. Personal communication.

Mutti, E., Luterbacher, H.P., Ferrer, J., Rosell, J., 1972. Schema stratigrafico e lineamenti di facies del Paleogene marino della Zona Centrale Sud-Pirenaica tra Tremp (Catalogna) e Pamplona (Navarra). Memorie della Società Geologica Italiana, 11, 391-416.

Mutti, E., Rosell, J., Allen, G.P., Fonnesu, F., Sgavetti, M., 1985. The Eocene Baronia tide-dominated delta-shelf system in the Ager basin. In: Mila, M.D., Rosell, J. (eds.). 6th European Regional Meeting of the International Association of Sedimentologists, Lleida (Spain), Excursion Guidebook, 579-600.

Mutti, E., Seguret, M., Sgavetti, M., 1988. Sedimentation and Deformation in the Tertiary Sequence of the Pyrenees. American Association of Petroleum Geologists Mediterranean Basin Conference, Field-Trip 7, Parma, University of Parma Special Publication, 153pp.

Mutti, E., Davoli, G., Mora, S., Sgavetti, M., 1994. The Eastern Sector of the South-Central Folded Pyrenean Foreland: Criteria for Stratigraphic analysis and Excursion Notes. Parma, University of Parma Special Publication, 244pp.

Mutti, E., Davoli, G., Tinterri, R., Zavala, C., 1996. The importance of ancient fluvio-deltaic systems dominated by catastrophic flooding in tectonically active basins. Memorie di Scienze Geologiche, 48, 232-291.

Mutti, E., Tinterri, R., Di Biase, D., Fava, L., Mavilla, N., Angella, S., Calabrese, L., 2000. Delta-front facies associations of ancient flood-dominated fluvio-deltaic systems. Revista de la Sociedad Geológica de España, 13(2), 165-190.

Mutti, E., Tinterri, R., Benevelli, G., Di Biase, D., Cavanna, G., 2003. Deltaic, mixed and turbidite sedimentation of ancient foreland basins. Marine and Petroleum Geology, 20, 733-755.

Pascual, J.O., Parès, J.M., Langereis, C.G., Zijderveld, J.D.A., 1992. Magnetostratigraphy and rock magnetism of the Ilerdian stratotype at Tremp, Spain. Earth and Planetary Interiors, 74, 139-157.

Pujalte, V., Schmitz, B., 2005. Revisión de la estratigrafía del Grupo Tremp («Garumniense», Cuenca de Tremp-Graus, Pirineos meridionales). Geogaceta, 38, 79-82.

Pujalte, V., Schmitz, B., Baceta, J.I., Orue-Etxebarria, X., Bernaola, G., Dinarès-Turell, J., Payros, A., Apellaniz, E., Caballero, F., 2009a. Correlation of the Thanetian-Ilerdian turnover of larger foraminifera and the Paleocene-Eocene thermal maximum: confirming evidence from the Campo area (Pyrenees, Spain). Geologica Acta, 7(1-2), 161-175.

Pujalte, V., Baceta, J.I., Schmitz, B., Orue-Etxebarria, X., Payros, A., Bernaola, G., Apellaniz, E., Caballero, F., Robador, A., Serra-Kiel, J., Tosquella, J., 2009b. Redefinition of the Ilerdian Stage (early Eocene). Geologica Acta, 7(1-2), 177-194.

Röhl, U., Bralower, T.J., Norris, R.D., Wefer, G., 2000. New chronology for the late Paleocene thermal maximum and its environmental implications. Geology, 28(10), 927-930.

Rosell, J., Linares, R., Llompart, C., 2001. El Garumniense prepirenaico. Revista de la Sociedad Geológica de España, 14(1-2), 47-56.

Rossi, C., 1997a. Organización secuencial de los depósitos fluviales y perimareales del Thanetiense de la Cuenca de Áger (Lérida). In: Calvo, J.P., Morales, J. (eds.). Avances en el conocimiento del Terciario Ibérico. Cuenca (Spain), 3er Congreso del Grupo Español del Terciario, Special Publication of the Universidad Complutense de Madrid, 189-192.

Rossi, C., 1997b. Microcodium y trazas fósiles de invertebrados en facies continentales (Paleoceno de la Cuenca de Áger, Lérida). Revista de la Sociedad Geológica de España, 10(3-4), 371-391.

Scheibner, C., Rasser, M.W., Mutti, M., 2007. The Campo section (Pyrenees, Spain) revisited: Implications for changing benthic carbonate assemblages across the Paleocene-Eocene boundary. Palaeogeography, Palaeoclimatology, Palaeoecology, 248, 145-168.

Schmitz, B., Pujalte, V., Nuñez-Betelu, K., 2001. Climate and sea-level perturbations during the Initial Eocene Thermal Maximum: evidence from siliciclastic units in the Basque Basin (Ermua, Zumaia and Trabakua Pass), northern Spain. Palaeogeography, Palaeoclimatology, Palaeoecology, 165, 299-320.

Schmitz, B., Pujalte, V., 2003. Sea-level, humidity, and land-erosion records across the initial Eocene thermal maximum from a continental-marine transect in northern Spain. Geology, 31(8), 689-692.

Schmitz, B., Pujalte, V., 2007. Abrupt increase in seasonal extreme precipitation at the Paleocene-Eocene boundary. Geology, 35(3), 215-218.

Selmo, E.M., 1993. Processi di dolomitizzazione nelle serie mesozoiche del Veneto e Trentino occidentali alla luce di uno studio geochimico-isotopico. Doctoral Thesis. Trieste, Università degli Studi di Trieste, unpublished.

Serra-Kiel, J., Canudo, J.I., Dinares, J., Molina, E., Ortiz, N., Pascual, J.O., Samsó, J.M., Tosquella, J., 1994. Cronoestratigrafía de los sedimentos marinos del Terciario inferior de la Cuenca de Graus-Tremp (Zona Central Surpirenaica). Revista de la Sociedad Geológica de España, 7(3-4), 273-297.

Serra-Kiel, J., Hottinger, L., Caus, E., Drobne, K., Ferràndez, C., Jauhri, A.K., Less, G., Pavlovec, R., Pignatti, J., Samsó, J.M.,

Schaub, H., Sirel, E., Strougo, A., Tambareau, Y., Tosquella, J., Zakrevskaya, E., 1998. Larger foraminiferal biostratigraphy of the Tethyan Paleocene and Eocene. Bulletin de la Societé Géologique de France, 169(2), 281-299.

Sluijs, A., Bijl, P.K., Schouten, S., Röhl, U., Reichart, G.J., Brinkhuis, H., 2011. Southern ocean warming, sea level and hydrological change during the Paleocene-Eocene thermal maximum. Climate of the Past, 7, 47-61.

Storme, J.I., Devleeschouwer, X., Schnyder, J., Cambier, G., Baceta, J.I., Pujalte, V., Di Matteo, A., Iacumin, P., Yans, J., 2012. The Palaeocene/Eocene boundary section at Zumaia (Basque-Cantabric Basin) revisited: new insights from high-resolution magnetic susceptibility and carbon isotope chemostratigraphy on organic matter (δ^{13}Corg). Terra Nova, 24, 310-317.

Svensen, H, Planke, S., Malthe-Sørenssen, A., Jamtveit, B., Myklebust, E., Rasmussen Eidem, T., Rey, S.S., 2004. Release of methane from a volcanic basin as a mechanism for initial Eocene global warming. Nature, 429, 542-545.

Thomas, E., Shackleton, N.J., 1996. The latest Paleocene benthic foraminiferal extinction and stable isotope anomalies. In: Knox, R.W.O'B., Corfield, R.M., Dunay, R.E. (eds.). Correlation of the Early Paleogene in Northwest Europe. London, Geological Society Special Publication, 101, 401-441.

Ullastre, J., Masriera, A., 1998. Nuevas aportaciones al conocimiento estratigráfico del Paleoceno continental del Pirineo catalán (España). Treballs del Museu de Geologia de Barcelona, 7, 95-128.

Waehry, A., 1999. Facies analysis and physical stratigraphy of the Ilerdian in the eastern Tremp-Graus basin. Terre et Environment, 15, 191pp.

Westerhold, T., Röhl, U., Laskar, J., Raffi, I., Bowles, J., Lourens, L.J., Zachos, J.C., 2007. On the durations of magnetochrons C24r and C25n and the timing of early Eocene global warming events: Implications from the Ocean Drilling Program Leg 208 Walvis Ridge depth transect. Paleoceanography, 22(2), 19pp.

Westerhold, T., Röhl, U., Raffi, I., Fornaciari, E., Monechi, S., Reale, V., Bowles, J., Evans, H.F., 2008. Astronomical calibration of the Paleocene time. Palaeogeography, Palaeoclimatology, Palaeoecology, 257, 377-403.

Wing, S.L., Harrington, G.J., Smith, F.A., Bloch, J.I., Boyer, D.M., Freeman, K.H., 2012. Transient Floral Change and Rapid Global Warming at the Paleocene-Eocene Boundary. Science, 310, 993-996.

Zachos, J.C., McCarren, H., Murphy, B., Röhl, U., Westerhold, T., 2010. Tempo and scale of late Paleocene and early Eocene carbon isotope cycles: Implications for the origin of hyperthermals. Earth and Planetary Science Letters, 299, 242-249.

Zamagni, J., Mutti, M., Ballato, P., Košir, A., 2012. The Paleocene-Eocene thermal maximum (PETM) in shallow-marine successions of the Adriatic carbonate platform (SW Slovenia). Geological Society of America Bulletin, 124(7-8), 1071-1086.

Manuscript received January 2013;
revision accepted November 2013;
published Online November 2013.